

Determination of the Pore Water Velocity Using a Salt Tracer Combined with Self-Potential Measurements

Huong Huynh Thi Thu*, Son Le Van, Hieu Tran Trong, Hai Lai Viet, Quang Nguyen Huu, Luan Phan Thi

Department of Tracer Techniques, Center for Applications of Nuclear Technique in Industry, Dalat, Vietnam

Email: *thuhuong9592@gmail.com

How to cite this paper: Thu, H. H. T., Van, S. L., Trong, H. T., Viet, H. L., Huu, Q. N., & Thi, L. P. (2023). Determination of the Pore Water Velocity Using a Salt Tracer Combined with Self-Potential Measurements. *Journal of Geoscience and Environment Protection*, 11, 15-27.

<https://doi.org/10.4236/gep.2023.111002>

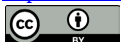
Received: December 22, 2022

Accepted: January 13, 2023

Published: January 16, 2023

Copyright © 2023 by author(s) and Scientific Research Publishing Inc. This work is licensed under the Creative Commons Attribution International License (CC BY 4.0).

<http://creativecommons.org/licenses/by/4.0/>



Open Access

Abstract

The tracer technique is recommended as an effective tool in surveying abnormal seepage through lakes and dams. By injecting a tracer into a known upstream location and monitoring the appearance of the tracer in the downstream leak point, it is possible to determine the direction and the average water velocity of the preferential flow through the dam. The detailed result achieved depends on the number of samples and the sampling locations to analyze tracer concentration over time in the field. This study proposes to use noninvasive self-potential measurements to determine the location and time the salt tracer moves through the seepage zone. The connection between the potential signal according to the propagation of the NaCl salt tracer and the water velocity was demonstrated through an experiment on a sandbox model. Experimental results express a good agreement between the time to reach the maximum value of the potential variation and the salt concentration variation with the time that water comes to monitoring locations. The result indicates an ability to determine the pore water velocity of the seepage zone based on the recording of potential signals produced by a salt tracer movement. The salt tracer test using NaCl combined with self-potential measurements was then applied to survey a leaking earth dam in the Dong Nai river basin (Vietnam).

Keywords

Earthen Dams, Tracer Technique, Leakage, Interstitial Velocity

1. Introduction

Leakage due to preferential seepage can gradually develop over time into ero-

sion, eventually destroying earth dams (Foster et al., 2000; Foster et al., 1998; Zhang et al., 2016). Once a dam has an abnormal seepage area downstream, the assessment of the seepage status plays a significant role in ensuring the safe operation of dams and reservoirs.

Hydrological techniques such as the observation of reservoir level and water leakage flux, stable isotope method, and hydrochemical method are qualitative methods, often performed in combination when a leakage point has just been detected (Ba, 2014; Kumar, 2013). Geophysical methods allow for determining the property distribution of the dam material (Al-Saigh et al., 1994; Di & Wang, 2010). Only the tracer method is an empirical technique that allows the determination of dynamic parameters such as flow direction, pore water velocity, and water travel time to describe the process of advection-dispersion of abnormal seepage flow (Hien & Khoi, 1996; Lee et al., 2007; Noraee-Nejad et al., 2021). Generally, a such tracer test is performed by introducing artificial tracers such as saline, ethanol, or fluorescent to a known location upstream and monitoring its concentration over time at target sites such as piezometers and leakage points downstream. The flow path and water velocity of preferential flow can be determined using the tracer appearance curves at the monitoring locations. It is easy to understand that the number of samples and the sampling locations for analyzing tracer concentration will determine the detail of the experimental results. For example, there were 26 observation wells with more than 30 water samples per well for tracer detection in sequential tracer tests conducted by Lee et al. (2007). Noraee-Nejad et al. (2021) conducted a tracer experiment using NaNO_3 salt with a total of 10 sampling points for the investigation of the Shahghasem dam. Therefore, unavailable sampling locations as well as cost issues due to the analysis of a large number of water samples are the limitation often faced. Recently, the detection of salt tracer movement through dams using nonpolarized electrodes on the ground is considered a way to overcome the above limitation. The principle is the variation in the total source current density generated by the transport of the salt tracer through preferential flow paths in a dam that can produce response electrical potential signals on the ground surface. Previous studies mainly focused on the localization of leakage flow by quantifying the variation of source current density generated by the movement of ions based on the inversion algorithm of self-potential data (Bolève et al., 2011; Ikard et al., 2012; Mao et al., 2015). However, these studies have not elucidated the relationships of the self-potential signal with tracer distribution along the preferential flow path during the transport process.

This work investigates the relationship between the potential signals according to the propagation of the NaCl salt tracer through the experiment on a physical model. Also, the applicability of the method to determine water velocity and flow direction with reasonable error is evaluated. A salt tracer test using NaCl combined with self-potential measurements was then applied to evaluate the direction and the velocity distribution of the preferential flow of an earth dam in the Dong Nai river basin (Vietnam).

2. Theoretical Background

In the tracer experiment, tracers are injected into known locations upstream, and then their occurrence at target sites downstream is monitored over time. The transport of the tracer in an underground environment is controlled by advection, hydrodynamic dispersion, and retention. Advection describes the bulk movement of particles along the mean direction of fluid flow at a rate equal to the average interstitial fluid velocity. Hydrodynamic dispersion refers to the spreading of the tracer in media contributed by molecular diffusion and mechanical dispersion resulting from variations in local velocities caused by microscopic heterogeneities of media (Sahimi et al., 1982). In this study, NaCl salt is used as a tracer. The retention process is ignored because chloride ion (Cl^-) dissociates in water from NaCl salt is a conservative indicator in the soil environment (Plata & Araguás, 2002).

Generally, the tracer breakthrough curve is bell-shaped (Figure 1). Previous studies have mentioned three concepts of time in the tracer curve: t_a —the arrival time, t_p —the peak time and t_r —the mean residence time. The mean residence of the tracer is

$$t_r = \int Ctdt / \int Cdt \quad (1)$$

where C is the tracer concentration.

The pore water velocity or the mean interstitial velocity of water is defined as the ratio between the Darcy velocity and the effective porosity. In general, the pore water velocity can be determined experimentally, as in

$$v^* = L/t \quad (2)$$

where L is the distance between injection and observation (m) and t is the time determined from the tracer breakthrough curve at the observation (s). Which t -concept in the tracer curve can be used depends on the actual flow conditions. The maximum velocity is determined from the arrival time and the average velocity is calculated from the peak time (Noraee-Nejad et al., 2021). The mean water velocity, however, is also evaluated from the mean residence time in groundwater investigations.

When a salt tracer such as NaCl solution is injected into the leakage zone increasing the ion concentration of the pore water, the source current density \vec{j}_s ($\text{A}\cdot\text{m}^{-2}$) generates the electrical potential (Revil & Linde, 2006).

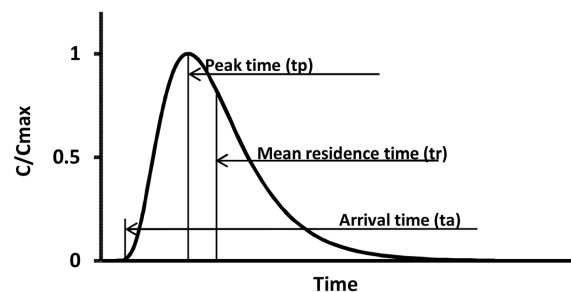


Figure 1. Examples of time characteristics of the tracer breakthrough curve: the arrival time, the peak time, and the mean residence time.

$$\vec{j}_s = \bar{Q}_v \vec{v} - \frac{K_b T}{Fe} (2t_{(+)} - 1) \nabla \sigma_f. \quad (3)$$

$$\nabla \cdot (\sigma \nabla \psi) = \nabla \cdot \vec{j}_s \quad (4)$$

where \vec{v} is the Darcy velocity (m/s); \bar{Q}_v is the excess charge density ($\text{C}\cdot\text{m}^{-3}$) which is determined from the equation $\log_{10} \bar{Q}_v = -9.2349 - 0.8219 \log_{10} k$, k is the permeability (m^2); $K_b = 1.381 \times 10^{-23}$ the Boltzmann constant ($\text{J}\cdot\text{K}^{-1}$); T is the absolute temperature (K); $F = \phi^{-m}$ is the formation factor, ϕ is the porosity; $e = 1.6022 \times 10^{-19}$ is the electron charge (C); $t_{(+)} = 0.38$ is the microscopic Hittorf number of the Na^+ in the pore water; $\sigma_f = \sigma F$ is the electrical conductivity of the pore water ($\text{S}\cdot\text{m}^{-1}$); σ is the electrical conductivity of the porous media ($\text{S}\cdot\text{m}^{-1}$); ψ (V) is the electrical potential. The self-potential signals are recorded using nonpolarizable electrodes located on the ground. The detection of tracer transport without sampling is a viable empirical approach, however, the link between the potential signal according to the propagation of the NaCl salt tracer and the water velocity needs to be considered.

3. Laboratory Experiment

3.1. Physical Model

The physical model used in this study is a rectangular box with dimensions of $61.6 \text{ cm} \times 30 \text{ cm} \times 30.8 \text{ cm}$ made of sheet glass with a thickness of 0.8 cm. The model is divided into three compartments by two 1 cm thick mica sheets with holes drilled 1 cm in diameter and a distance between holes of 2 cm. Two 10 cm long compartments at the ends act as upstream and downstream reservoirs, while the 38 cm long compartment in the middle is packed with glass beads. Fabric mesh with a mesh diameter of 100 μm is attached to the two shields to prevent glass beads from spilling into the other two compartments. The total height of the glass bead column is 20 cm. The porosity of the middle compartment is 37%. The flow through the porous media is controlled by the water levels of the upstream and downstream. Upstream water is supplied by a water tank located 3 m above the ground and a tube with a diameter of 1 cm. The supplying flow rate is regulated with a valve. The downstream water level is adjusted by changing the outlet height of the 1 cm diameter overflow discharge tube. The experiment used tap water as the fluid with an average conductivity of $2.4 \times 10^{-3} \text{ S}\cdot\text{m}^{-1}$. We used laboratory glass beads with a diameter of about 450 - 500 μm . By measuring the outlet flow rate according to the difference in water level, the permeability is determined as $1.95 \times 10^{-10} \text{ m}^2$. The experimental system and the sketch of the physical model are shown in **Figure 2(a)** and **Figure 2(b)**.

The laboratory Cu/CuSO₄ electrodes, in combination with a Fluke 87 V voltmeter (USA), were used to record the electrical potential during the transport of the NaCl tracer. The in-house electrodes operate with a natural drift of 0.02 mV/min (22°C). The dependence of the potential drift on ambient temperature is ignored because the temperature fluctuation in the experiment is insignificant (within 0.1°C). A total of 3 electrode arrays (4 electrodes each array) were inserted

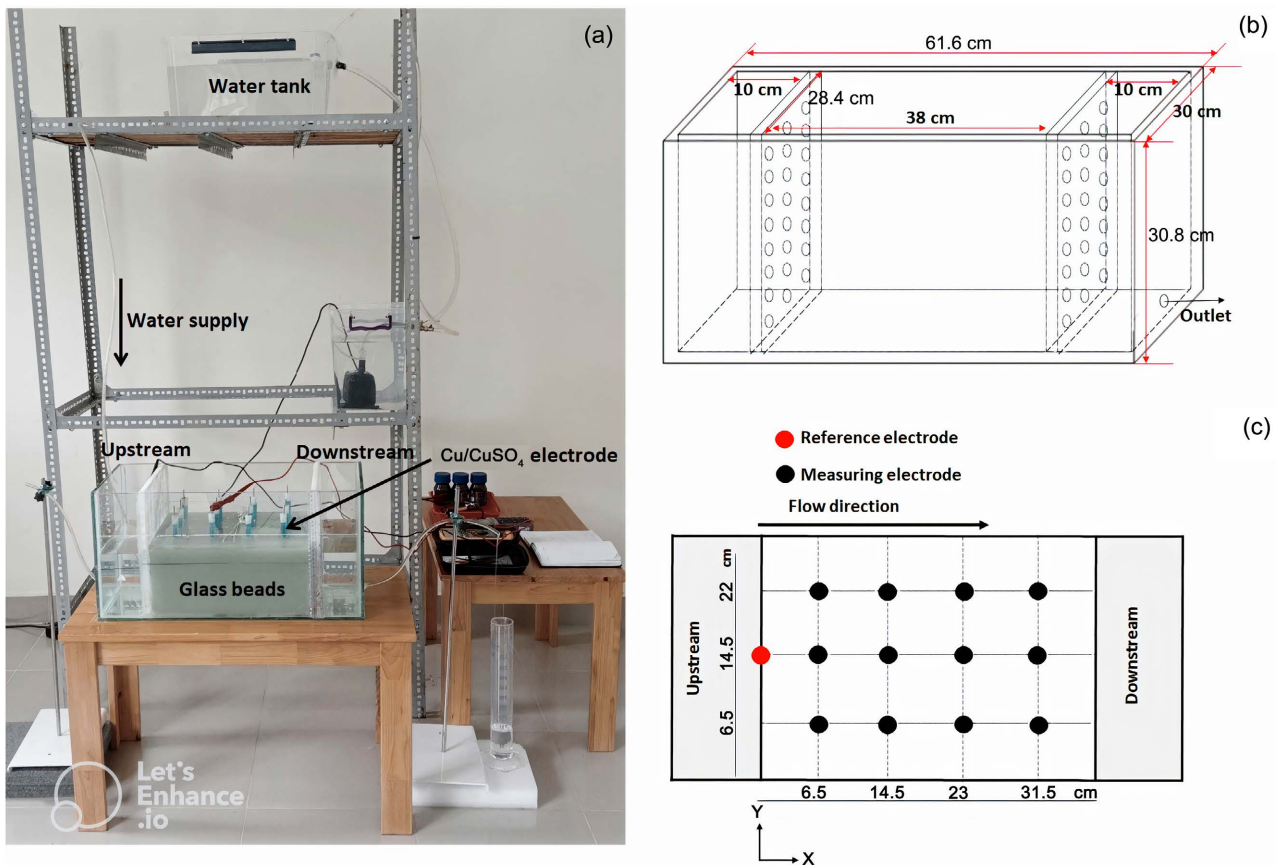


Figure 2. The experimental system: (a) Photo of experimental system; (b) Sketch of physical model; (c) Illustration of electrode position (top view).

into the middle compartment (depth 8.5 cm from the top), and the reference electrode was placed upstream ($x; y$) = (0 cm; 14.5 cm). The position of the electrodes is considered in the Cartesian coordinate system with the x-axis parallel to the flow direction, and the y-axis perpendicular to the flow direction. The electrode arrays have coordinates y = (6.5 cm; 14.5 cm; 22 cm), with the positions of the measuring electrodes along the x-axis being (6.5 cm; 14.5 cm; 23 cm; 31.5 cm) as shown in **Figure 2(c)**.

3.2. Experimental Procedure

The upstream level was maintained at 20 cm. The tracer experiment was performed with a flow rate of 0.61 L/min corresponding to a 19 cm downstream level. The pore water velocity was 2.90 cm/min. The temperature during the experiment was stable in the range of 22°C. We injected the NaCl tracer and monitored the self-potential signal over time for the first stage. The next stage repeats the tracer injection under same conditions and determines the Cl^- concentration at the monitoring locations.

- **First stage.** After setting the downstream and upstream levels, the experimental system was kept in a stable state for several hours. Before the tracer injection, the potential difference between the 12 measuring electrodes and

the reference electrode was recorded, which includes the signal generated by the steady flow in the model and the difference in internal potential between the electrodes. Simultaneously, the initial conductivity of the water is also measured to get the background value. 120 mL of the salt tracer solution (containing 4.42 g of NaCl) was injected into the upstream reservoir. The water volume of the upstream reservoir was 5.68 L. The potential difference between the reference electrode and measuring electrodes was recorded over time using a Fluke 87 V voltmeter (USA). The measuring time for 12 electrodes was 20 s, the measurement frequency was 1 min. The NaCl concentration over time at the downstream drainage was measured using a conductivity quantity using a Hanna HI98197 device (Romania). The linear relationship of the concentration of Cl^- (C, mg/L) and the conductivity of water (EC, $\mu\text{S}/\text{cm}$) are shown by the equation $C = 0.25\text{EC} - 4.49$ ($R^2 = 0.998$). The initial electrical potential before tracer injection and the natural drift potential were removed from the measurement. After about 60 minutes of experimentation, the electrodes were removed from the model, and continuously running tap water through the model for several days to wash away any remaining salt.

- **Second stage.** The tracer injection was repeated under the same condition as the previous stage, using 1 mL syringes to collect water samples at the electrode locations $y = 14.5$ cm and $x = [6.5$ cm; 14.5 cm; 23 cm; 31.5 cm] over time. The water samples were then analyzed for Cl^- concentration at the Laboratory (VILAS-609) of the Center for Applications of Nuclear technique in Industry. The concentration of Cl^- in water was quantified according to the test method TCVN 6494-1:2011 with a detection limit of 0.01 mg/L. The purpose is to determine the experimental tracer curve at the electrode placement sites. Besides, the upstream water conductivity was also observed over time to confirm the repeatability of the inlet boundary condition of the seepage zone.

4. Field-Scale Test

The main aim of the experiment is to determine the velocity distribution of the preferential flow of an earth dam in the Dong Nai river basin (Vietnam) using the tracer technique combined with self-potential measurements.

The study dam was built in 1997 in the Dong Nai river basin. The dam is situated about 200 km northeast of Ho Chi Minh City. The study dam is a homogeneous earth dam of 36 m in height and a crest length of 215 m. According to the company's report, the leak area appears downstream of the dam when the reservoir water level reaches a value greater than 604 m. The size of the downstream leak zone is about 7 m \times 3 m at an elevation of 595 m (**Figure 3(a)**). In December 2021, we collaborated with the dam supervisor to create a ditch to collect seepage water into a hole with dimensions of 40 cm \times 40 cm \times 15 cm in order to measure the leak flow rate. The results show that the leakage flow was 0.5 L/min when the lake water level reached 605 m.

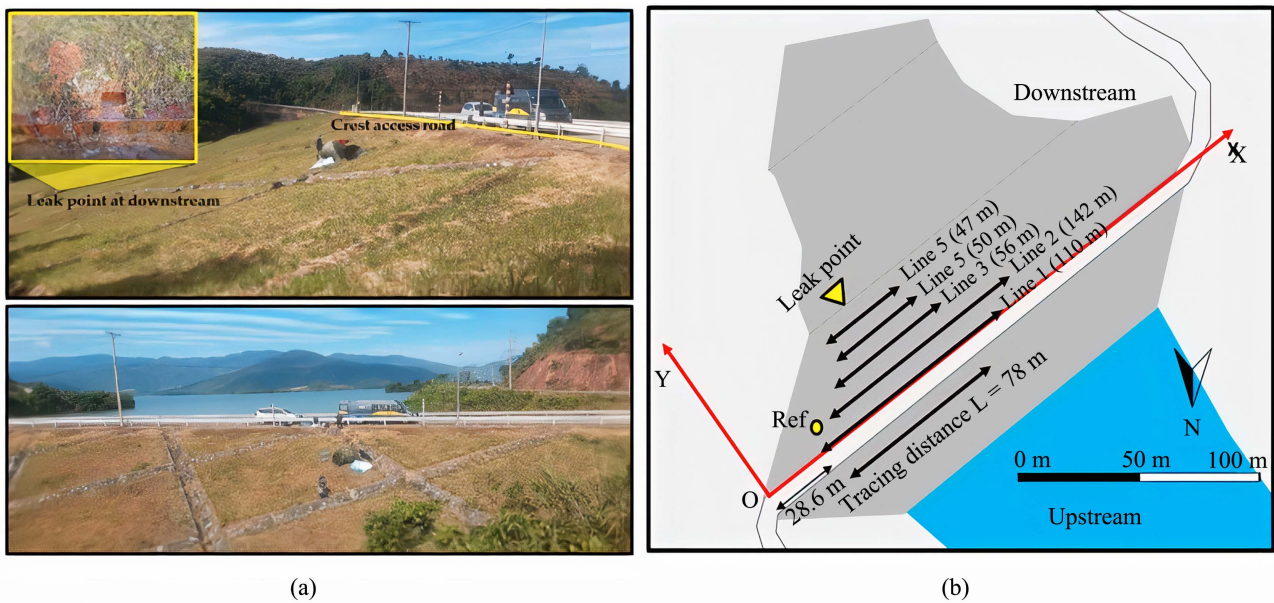


Figure 3. (a) The study dam site; (b) The tracing distance, measuring lines for electrical potential (Line 1 - 5), and reference electrode (Ref) position.

The salt tracer test was conducted to determine the direction and local pore water velocity of the preferential flow through the dam. Nylon bags containing the NaCl tracer in crystal form were introduced into the reservoir on December 18, 2021. The tracing distance was 78 m, symmetrical to the leak site (**Figure 3(b)**). The bags were perforated so that the salt crystal could dissolve into the reservoir water at a certain rate. Each 5 kg NaCl bag was placed at a depth of 1 m and spaced 3 m apart. The reservoir water level at the time of tracer injection was 604.6 m. The electrical conductivity and Cl^- concentration of the reservoir water according to the distance were determined over a time of about 3 hours from the injection point. The leak point was the only location where we could sample the downstream. The leak water samples were collected until February 3, 2022, to analyze the conductivity and Cl^- concentration at the Laboratory (VILAS-609) of the Center for Application of Nuclear techniques in Industry. Water samples having a volume of 300 mL were filled in sealed plastic bottles to avoid contact with air. The Cl^- concentration of samples was determined according to the test method TCVN 6494-1:2011 with a minimum detection limit of 0.01 mg/L. The electrical conductivity of the samples was measured using a Hanna HI98197 instrument (Romania) with a resolution of 0.1 $\mu\text{S}/\text{cm}$. Before the injection, the concentration of Cl^- in the reservoir water was 3.80 mg/L and in the leak water, it was 2.77 mg/L, corresponding to the conductivity of 66.5 $\mu\text{S}/\text{cm}$ and 28.5 $\mu\text{S}/\text{cm}$.

A total of 5 measuring lines for electrical potential (Line 1 - 5) were carried out at the dam site before tracer injection (December 17, 2021) and after tracer injection (January 5, 2022, January 18, 2022, January 26, 2022). The measuring lines were parallel to the toe of the dam downstream and were 10 m apart. The length of the measuring lines was designed to be reduced to the downstream in

order to save survey time. Measurements were performed using a pair of Cu/CuSO₄ non-polarized electrodes connected to a measuring device with a maximum impedance of 20 MΩ using a 500 m cable (ARES II measurement system, GF Instruments). In this study, the reference electrode was fixed at the left abutment of the dam (Figure 3(b)), and the other electrode was moved to each measurement point on the measuring lines. The average distance of the measuring points was 8 m, however, the locations of the measuring points were adjusted according to the ground surface conditions at the site. At each location, a small hole was dug to contact moist soil. The average depth of each hole was about 10 cm. Because of the sensitivity of the Cu/CuSO₄ electrodes to temperature changes, the electrodes were shielded from sunlight during measurement with a pre-measurement waiting time of 5 min for each measurement point. At each measurement point, 5 measurements were performed with an average relative error of 1.7%. At the beginning and end of each measuring line, the drift potential of the two electrodes was determined when they were placed in a bath of saturated CuSO₄ solution. The potential value of which was about 1 mV. Previous studies have shown that telluric current correction can be neglected with measurements taken over a short-time period and site scales below 1 km (Revil et al., 2003). The raw electrical potential data were then corrected for the drift potential for each measuring line.

5. Results and Discussion

5.1. Laboratory Experiment

The conductivity of upstream and downstream water over time in both experimental periods is shown in Figure 4. The results show the repeatability of the boundary condition upstream. The water conductivity upstream declines with time due to the dilution effect with a water flow rate of 0.61 L/min. The water conductivity downstream over time is bell-shaped, and a percentage of salt recovery of 99.8% is observed.

The Na⁺ and Cl⁻ ions dissociated from the NaCl salt move with the injected water and pass through the monitoring locations of $x = 6.5$ cm, 14.5 cm, 23 cm, and 31.5 cm. The transport of ions in water through pore spaces increases the

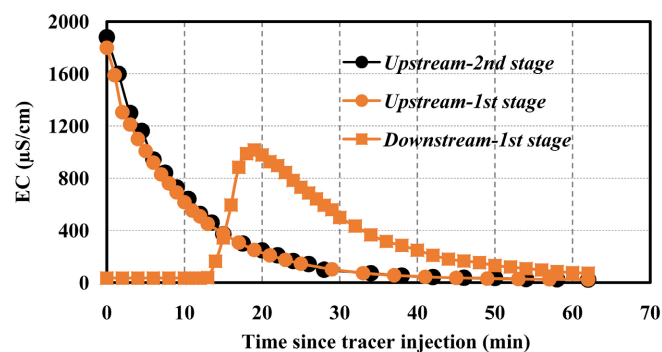


Figure 4. The conductivity of upstream and downstream water over time in both experimental periods.

conductivity of the water at monitoring locations, and simultaneously, generates self-potential signals. Immediately after the injection, the self-potential at measuring positions ($x = 6.5$ cm, 14.5 cm, 23 cm, and 31.5 cm) drops to a negative value, then suddenly crosses zero and is almost stable during experimental time.

Figure 5 presents the distribution of NaCl concentration and self-potential at the monitoring site according to normalized time ($t.v^*/L$), $v^* = 2.90$ cm/min, $L = \{6.5$ cm, 14.5 cm, 23 cm, and 31.5 cm}. The results show that the time to reach the maximum concentration corresponds to the peak time of the potential signal. The travel time of water ($t.v^*/L = 1$) is earlier than the time to reach the maximum concentration due to the tracer dispersion effect.

The reasonable between the time to reach the maximum value of the potential variation and the salt concentration variation with the time that water comes to monitoring locations is shown in **Figure 6**. The time to reach the maximum potential variation are 2 min ($x = 6.5$ cm), 7 min ($x = 14.5$ cm), 10 min ($x = 23$ cm), and 13 min ($x = 31.5$ cm). The tracer curve is affected by the movement of the tracer along the mean direction of fluid flow, as well as, the hydrodynamic dispersion process. Therefore, it can be seen that the advection related to fluid flow velocity is the dominant process when the maximum potential variation achieves. The pore water velocity can be determined based on the time of maximum potential variation (i.e. potential anomaly). The average error of the calculated velocity (2.5 cm/min) is about 13% compared with the reference value (2.9 cm/min).

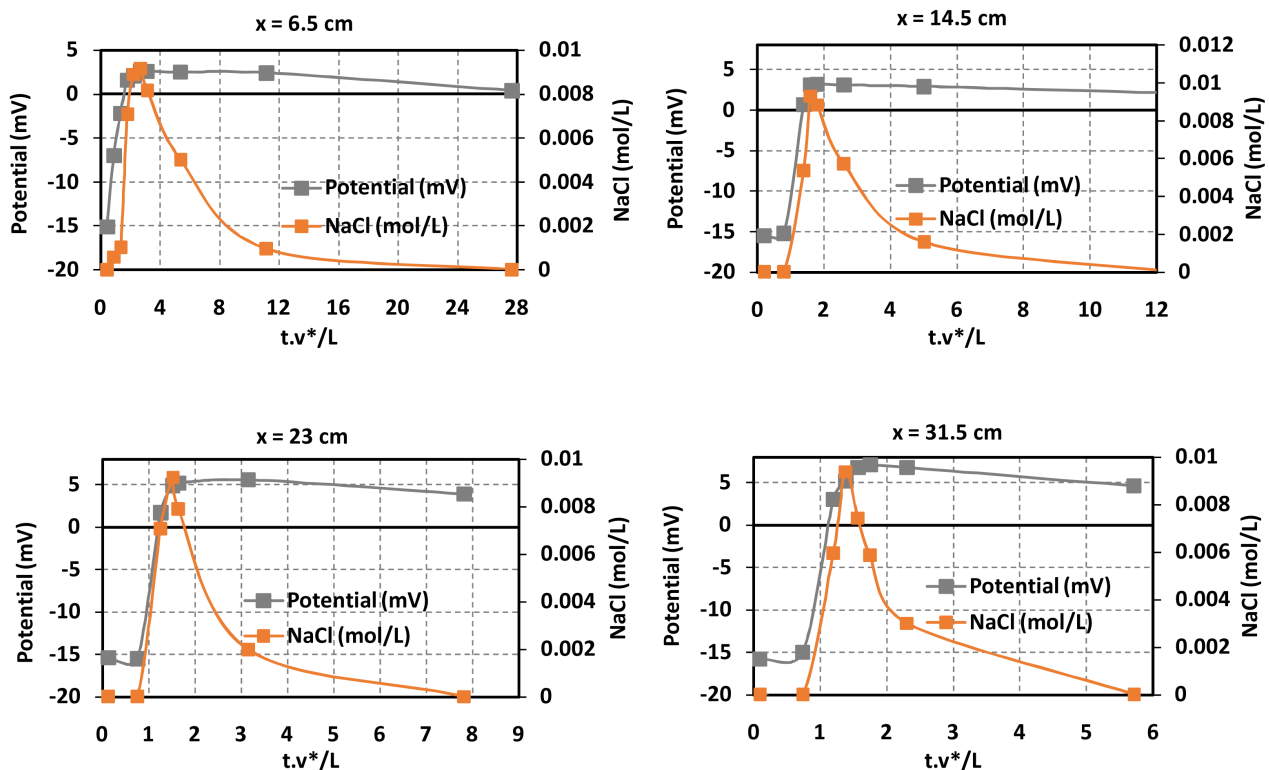


Figure 5. Experimental tracer concentration (NaCl, mol/L) and potential (mV) over time at monitoring sites.

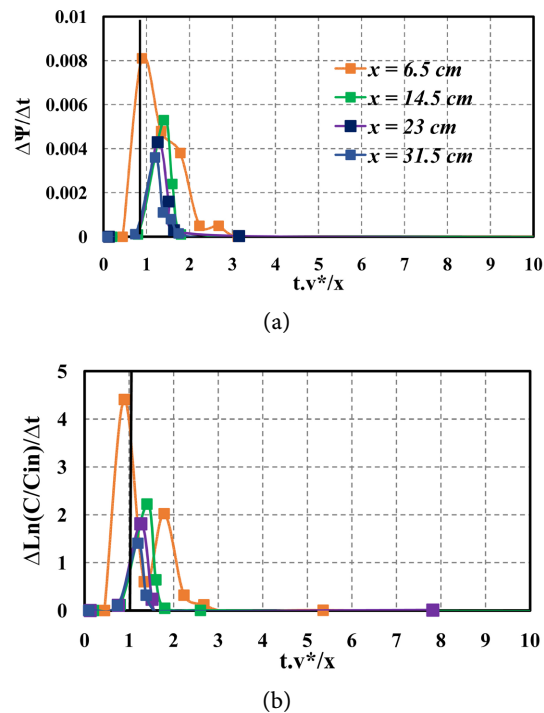


Figure 6. The reasonable between the time to reach the maximum potential variation (a) and salt concentration variation with the time travel of water (b).

5.2. Field-Scale Experiment

The NaCl tracer was introduced into the reservoir water at an elevation of 604.5 m. Measurement results of electrical conductivity and Cl^- concentration in the reservoir water at 0.8 hours, 1.8 hours, 2.8 hours, and 3.3 hours after injection are presented in **Figure 7(a)**. The purpose is to locate the inlet of seepage leakage of the dam. The inlet was determined as the point with the highest concentration of tracer after a period of diffusion. The measurement results show that the conductivity and Cl^- concentration peaked at about 42 m from the zero distance injection. After 3.3 hours, the conductivity of the reservoir water was once again close to the background value.

The analysis results of electrical conductivity and Cl^- concentration in water at the leak point are shown in **Figure 7(b)**. The response tracer curve is in the form of a single peak, peaking after 40 days of the injection. The maximum conductivity value is 118.70 $\mu\text{S}/\text{cm}$ corresponding to the maximum Cl^- concentration of 28.06 mg/L.

Figure 8 presents the results of electrical potential anomalies at the dam after 18 days, 30 days, and 40 days since the injection. The location of the anomaly that indicates the direction of tracer movement from upstream to the leak point has a horizontal V-shape. The travel time of the salt tracer from upstream (position 1) to Line 2 (position 2) is 18 days, from Line 2 (position 2) to Line 5 (position 3) is 12 days, and from Line 5 (position 3) to the leak point is 10 days. Based on the distances of movement, the local pore water velocity is presented in **Table 1**. The value of local pore water velocity ranges from 1.2×10^{-5} m/s to 7.0×10^{-5}

m/s. The calculation results show that the velocity in the 2 - 3 position range is the greatest. Taking into account the tortuosity of the porous medium, the actual velocity of the water is proportional to the actual distance travelled $L_a = L\tau$, τ is the tortuosity. The actual velocity results are presented as **Table 1** with $\tau = 1.4$ (Freeze & Cherry, 1979).

Table 1. Local pore water velocity along the preferential flow of the study dam.

Position	Travel distance (m)	Travel time (days)	Pore water velocity (m/s)	Actual pore water velocity (m/s)
1 - 2	77.8	18	5.0×10^{-5}	7.0×10^{-5}
2 - 3	73	12	7.0×10^{-5}	9.9×10^{-5}
3-Leak point	10.4	10	1.2×10^{-5}	1.7×10^{-5}

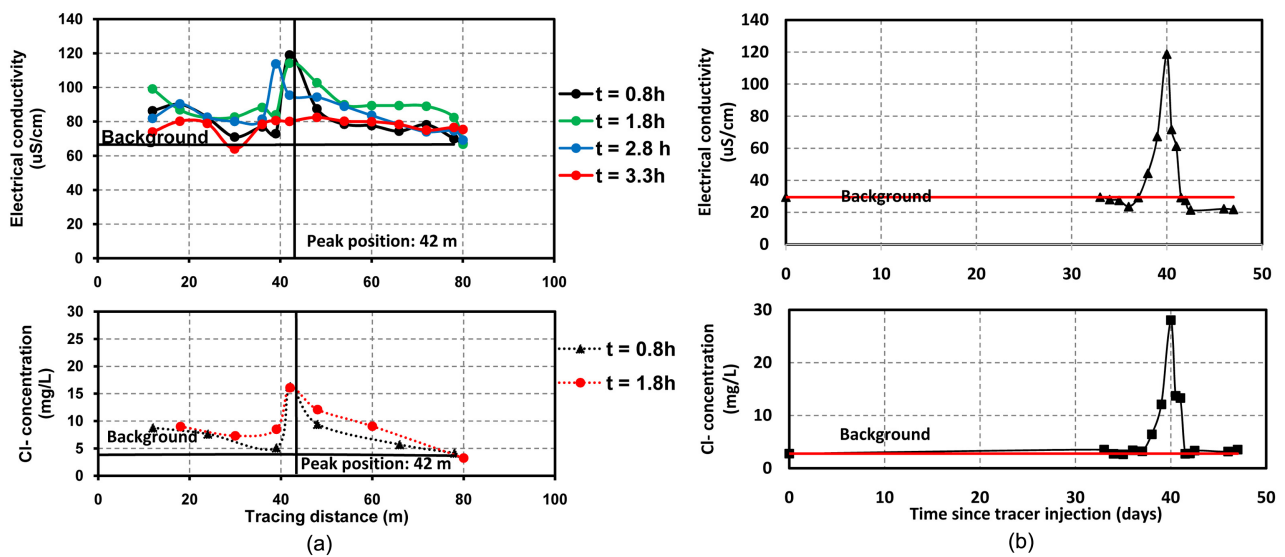


Figure 7. Results of salt tracer test at the study dam: (a) Measurement results of electrical conductivity and Cl^- concentration in reservoir water at 0.8 h, 1.8 h, 2.8 h and 3.3 h after injection; (b) Electrical conductivity and Cl^- concentration in water at the leak point over time.

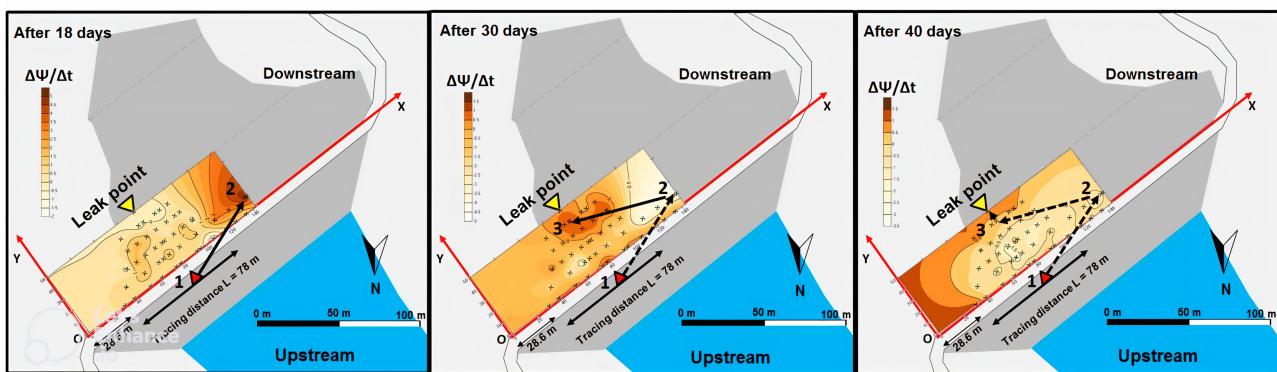


Figure 8. Location of electrical potential anomalies ($\Delta\Psi/\Delta t$) at the study dam after injection: 18 days, 30 days, and 40 days. Position 1 is conventionally the leakage inlet, determined at the point where the conductivity or Cl^- concentration peaks after injection.

6. Conclusion

The study focused on evaluating the reasonable between the self-potential anomalies and salt concentration distribution, which has not been addressed in previous studies. The obtained results allow the assessment of water velocity in a preferential flow path with an error of about 13%. A field-scale salt tracer experiment combined with self-potential measurements was performed at a leaking earth dam in Vietnam to illustrate the applicability of the method. The tracer response curve at the leak site shows that the transport time of the seepage water is approximately 40 days. The electrical potential anomaly after 18 days, 30 days, and 40 days, since tracer injection, indicates the path of the preferential flow from upstream to the leak point with the local pore water velocity in the range of 1.7 to 9.9×10^{-5} m/s.

The achieved results show that the approach will be very useful for assessing internal erosion due to seepage inside the earthen dam based on the criterion of pore water velocity. In addition, this technique presents an outstanding advantage in terms of testing costs as well as overcoming difficulties associated with sampling for tracer analysis in the field site.

Acknowledgements

This work was supported by the project ĐTCB.01/20/TTUDKTHN under the grant of the Vietnam Ministry of Science and Technology.

Conflicts of Interest

The authors declare no conflicts of interest regarding the publication of this paper.

References

- Al-Saigh, N. H., Mohammed, Z. S., & Dahham, M. H. (1994). Detection of Water Leakage from Dams by Self-Potential Method. *Engineering Geology*, *37*, 115-121. [https://doi.org/10.1016/0013-7952\(94\)90046-9](https://doi.org/10.1016/0013-7952(94)90046-9)
- Ba, J. F., Zhan, L. C., & Zhang, B. (2014). Isotope Analysis on the Recharge Source of the Leakage Water behind the Right Dam of Suzhi Hydroelectric Station. *Advanced Materials Research*, *1015*, 581-584. <https://doi.org/10.4028/www.scientific.net/AMR.1015.581>
- Bolève, A., Janod, F., Revil, A., Lafon, A., & Fry, J.-J. (2011). Localization and Quantification of Leakages in Dams Using Time-Lapse Self-Potential Measurements Associated with Salt Tracer Injection. *Journal of Hydrology*, *403*, 242-252. <https://doi.org/10.1016/j.jhydrol.2011.04.008>
- Di, Q., & Wang, M. (2010). Determining Areas of Leakage in the Da Ye Dam Using Multi-Electrode Resistivity. *Bulletin of Engineering Geology and the Environment*, *69*, 105-109. <https://doi.org/10.1007/s10064-009-0222-1>
- Foster, M. A., Spannagle, M., & Fell, R. (1998). *Report on the Analysis of Embankment Dam Incidents*. UNICIV Report No. R-374, University of New South Wales.
- Foster, M., Fell, R., & Spannagle, M. (2000). The Statistics of Embankment Dam Failures and Accidents. *Canadian Geotechnical Journal*, *37*, 1000-1024.

<https://doi.org/10.1139/t00-030>

- Freeze, R. A., & Cherry, J. A. (1979). *Groundwater*. Prentice-Hall.
- Hien, P. D., & Khoi, L. V. (1996). Application of Isotope Tracer Techniques for Assessing the Seepage of the Hydropower Dam at Tri An, South Vietnam. *Journal of Radioanalytical and Nuclear Chemistry*, 206, 295-303. <https://doi.org/10.1007/BF02039656>
- Ikard, S. J., Revil, A., Jardani, A., Woodruff, W. F., Parekh, M., & Mooney M. (2012). Saline Pulse Test Monitoring with the Self-Potential Method to Nonintrusively Determine the Velocity of the Pore Water in Leaking Areas of Earth Dams and Embankments. *Water Resource Research*, 48, W04201. <https://doi.org/10.1029/2010WR010247>
- Kumar, C. P. (2013). Hydrological Studies Using Isotopes. *International Journal of Innovative Research & Development*, 2, 8-15.
- Lee, J.-Y., Kim, H.-S., Choi, Y.-K., Kim, J.-W., Cheon, J.-Y., & Yi, M.-J. (2007). Sequential Tracer Tests for Determining Water Seepage Paths in a Large Rockfill Dam, Nakdong River Basin, Korea. *Engineering Geology*, 89, 300-315. <https://doi.org/10.1016/j.enggeo.2006.11.003>
- Mao, D., Revil, A., Hort, R. D., Munakata-Marr, J., Atekwana, E. A., & Kulesa, B. (2015). Resistivity and Self-Potential Tomography Applied to Groundwater Remediation and Contaminant Plumes: Sandbox and Field Experiments. *Journal of Hydrology*, 530, 1-14. <https://doi.org/10.1016/j.jhydrol.2015.09.031>
- Noraee-Nejad, S., Sedghi-Asl, M., Parvizi, M., & Shokrollahi, A. (2021). Salt Tracer Experiment through an Embankment Dam. *Iranian Journal of Science and Technology. Transactions of Civil Engineering*, 45, 2787-2797. <https://doi.org/10.1007/s40996-021-00714-8>
- Plata, B. A., & Araguás, A. L. (2002). *Detection and Prevention of Leaks from Dams*. A. A. Balkema Publishers.
- Revil, A., & Linde, N. (2006). Chemico-Electromechanical Coupling in Microporous Media. *Journal of Colloid and Interface Science*, 302, 682-694. <https://doi.org/10.1016/j.jcis.2006.06.051>
- Revil, A., Naudet, V., Nouzaret, J., & Pessel, M. (2003). Principles of Electrography Applied to Self-Potential Electrokineticsources and Hydrogeological Applications. *Water Resources Research*, 39, 1114. <https://doi.org/10.1029/2001WR000916>
- Sahimi, M., Heiba, A. A., Hughes, B. D., Ted Davis, H., & Scriven, L. E. (1982). Dispersion in Flow through Porous Media. In *SPE Annual Technical Conference and Exhibition* (No. SPE-10969-MS). <https://doi.org/10.2118/10969-MS>
- Zhang, L., Peng, M., Chang, D., & Xu, Y. (2016). *Dam Failure Mechanisms and Risk Assessment*. John Wiley & Sons Singapore Pte. Ltd. <https://doi.org/10.1002/9781118558522>